19th Brazilian Congress of Thermal Sciences and Engineering
November 6th–10th, 2022, Bento Gonçalves - RS - Brazil

ENC-2022-0053
NUMERICAL MODELLING OF MICRO-SCALE LIQUID-LIQUID DISPLACEMENT IN HOMOGENEOUS AND HETEROGENEOUS POROUS MEDIA

Ayrton Cavallini Zotelle
Edson José Soares
LABREO, Department of Mechanical Engineering, Universidade Federal do Espírito Santo, Avenida Fernando Ferrari, 514, Goiabeiras, Vitória, ES, 29075-910, Brazil
ayrton.zotelle1@hotmail.com
edson.soares@ufes.br

Renato do Nascimento Siqueira
LPMF, Department of Mechanical Engineering, Instituto Federal do Espírito Santo - campus São Mateus, Rod. BR 101 norte, km 58, Litorâneo, São Mateus, ES, 29932-540, Brazil
renatons@ifes.edu.br

Abstract. *The displacement of one liquid by another is a fundamental fluid mechanics problem with many applications, such as the oil displacement in petroleum reservoirs. The oil recovery occurs typically in three stages. In the primary stage, the oil is produced by the internal pressures of the reservoir. Studies show that a small amount of oil is recovered in this stage, around 10%. In the second stage, generally, oil is recovered by injection of a Newtonian fluid (water or gas), resulting in an additional recovery. The residual oil that remains trapped in the porous after the secondary stage is still significant, on average, more than 50% of the original oil in geological reservoir. In the third stage (enhanced oil recovery), it is common to use polymer solutions after water-flooding, which can recover a significant additional amount of oil by changing the interfacial interaction between the fluids. Concerning Newtonian fluids injection, the dimensionless parameter that have more influence on the recovery process are the capillary number (Ca) and the viscosity ratio (N_μ). This study uses numerical simulation to evaluate the influence of the capillary number and viscosity ratio on the displacement efficiency and the interfacial behaviour of a liquid-liquid displacement. The open source software Basilisk© has been applied in many studies, especially those that evaluate interfacial phenomena, and for that reason, it was used as the solver for the simulations in this paper. The software uses Cartesian adaptive meshes, which allows the refinement of the fluids and solid interfaces to accurately track its position. The numerical model is a simplified micro-scale porous media, with homogeneous and heterogeneous disposition of grains in order to evaluate the heterogeneity effects on the oil recovery. The preliminary results show that the injection of a more viscous fluid have a better displacement efficiency on either homogeneous and heterogeneous porous media, and the capillary number can have different behaviours, depending of the grains disposition. Normally, the heterogeneous porous media retain more oil than the homogeneous one due to the existence of preferential paths in low resistance locations.*

Keywords: *Interfacial phenomena, Viscosity ratio, Capillary number, Homogeneous porous media, Heterogeneous porous media*

1. INTRODUCTION

The displacement of one liquid by another is a fundamental fluid mechanics problem with many applications such as the oil displacement in petroleum reservoir. The oil recovery occurs typically in three stages. In the preliminary stage, the oil is produced by the internal pressures of the well. A small amount of oil is recovered in this stage, around 10 %. In the second stage, generally, oil is recovered by injection of a Newtonian liquid (water or gas), resulting in an additional of recovery of 20–40%. The residual oil that remains trapped in the porous after the secondary stage is significant, on average, more than 50 % of the original oil in geological reservoir. In the third stage (enhanced oil recovery), it is common to use polymer solutions after water-flooding, which can recover a significant additional amount of oil (Needham and Doe, 1987; Fathi *et al.*, 2011).

Since the displacement velocities are very slow and the viscosity involved are quite large, typically, these processes occur with negligible inertial effects. Still, other parameters such as the Capillary number (Ca) and Viscosity ratio (N_μ) can play a fundamental role in the physics of the phenomena. Remarkable contributions in an attempt to understand the role played by Ca come from Taylor (1960, 1961) who analyses the gas-liquid displacement in capillary tubes and plane surfaces, which is a rough approximation of a real porous media. Mainly, the author shows that the fraction of mass attached to the wall at the breakthrough increases with Ca. Soares *et al.* (2005) and Soares and Thompson (2009) study the displacement of a viscous liquid by other. The authors show that when the viscosity of the injected fluid increases relatively to the displaced one, at the same Ca, the interface tip thins, but the lost mass reduce by the increase of the viscous drag.

Lenormand *et al.* (1988) conducted several simulations and experiments on immiscible liquid displacement in porous media. The authors describe physically the relative importance of Ca and N_μ, which characterise three different domains concerned with liquid displacement, called phase diagram. The three domains are called: *stable displacement*; *viscous fingering*; and *capillary fingering*. The stable displacement is characterized by negligible capillary force and low viscosity ratio, i.e. the injected fluid is more viscous than the recovered one. In this state, the main force is due to the viscosity of the injected fluid. The interface front is flat, with some irregularities, and the trapped liquid fraction is very small. The viscous fingering is also characterized by the negligible capillary number but high viscosity ratio. The main force is due to the viscosity of the displaced fluid. The fingers spread across the entire porous media, which turns the sweep efficiency very low. Finally, the capillary fingering is characterized by high capillary force (low capillary number). The fingers also spread across the porous media, but the sweep efficiency is significantly larger than that of the viscous fingering. These three fingering regimes in porous media were also observed by different researchers (Zhang *et al.*, 2011; Tsuji *et al.*, 2016; Hu *et al.*, 2020).

A fluid displacement in a porous media is quite complex. Most of the works that study the phenomena use a simplified model, in which the governing equations are not fully computed to simulated the flow (Dias and Payatakes, 1986). With the advance of numerical methods for interfacial dynamics, direct numerical simulations (DNS) have been conducted for multiphase flow in porous media. Two interesting works are those of Shende *et al.* (2021) and Zhong *et al.* (2018), where the authors use DNS to determine lost mass fraction of a two-phase flow in porous media, but some details are still missing.

The Basilisk© software is a open source code to solve differential partial equations using the Finite Volume Method (FVM) developed on Centre National de la Recherche Scientifique (CNRS) based at Institut Jean le Rond ∂'Alembert of Sorbonne Université, Paris - France (Popinet, 2009, 2015; Lagrée *et al.*, 2011). This solver has been used for diverse flows, especially those with interfacial dynamics, by different researchers (Lagrée *et al.*, 2011; Deka *et al.*, 2019; Pierson *et al.*, 2020; Deka *et al.*, 2020; Deoclecio *et al.*, 2021), and was also applied on our simulations. This research conduct numerical simulations of immiscible liquid-liquid displacement in a homogeneous and heterogeneous porous media composed of spheres and analyses the interface propagation considering its details with the changes of the operational parameters, i.e., the shape of its front and the film of the displaced liquid attached to the spheres for different N_μ and Ca.

2. METHODOLOGY

This paper use the Basilisk© software to simulate a multiphase interaction between two fluid phases and one solid phase on a recovery process in a porous media. The fluids and solid interaction were modelled using the embedded boundary method (more details at Johansen and Colella (1998)). The fluids interaction was modelled using the Volume of Fluid (VOF). This model treat the phases as continuous and immiscible, solving a unique continuity and momentum equation to the both phases, also called one-fluid method, and track the interface around the domain by solving the advenction equation to the volume fraction (f) of the primary phase:

$$\frac{\partial f}{\partial t} + \boldsymbol{u} \cdot \nabla f = 0 \,, \tag{1}$$

in which $\boldsymbol{u}$ is the velocity vector. The mass also need to be conserved in the flow. Considering a incompressible flow, the continuity equation to a one-fluid method is:

$$\nabla \cdot \boldsymbol{u} = 0 \,, \tag{2}$$

and the momentum equation, considering the multiphase flow with the surface tension interaction is:

$$\rho \left(\frac{\partial \boldsymbol{u}}{\partial t} + \boldsymbol{u} \cdot \nabla \boldsymbol{u} \right) = -\boldsymbol{\nabla} P + \nabla \cdot \left[\mu \left(\nabla \boldsymbol{u} + \nabla \boldsymbol{u}^T \right) \right] + \sigma \kappa \delta_d \, . \boldsymbol{n} \,, \tag{3}$$

where $\rho = f\rho_1 + (1-f)\rho_2$ is the average fluid density, $\boldsymbol{\nabla} P$ is the pressure gradient, $\mu = f\mu_1 + (1-f)\mu_2$ is the average fluid viscosity, σ is the surface tension, κ is the interface curvature, δ_d is the Dirac delta function and $\boldsymbol{n}$ is the interface unitary normal vector, calculate as:

$$\boldsymbol{n} = -\frac{\nabla f}{|\nabla f|} \,. \tag{4}$$

The interface curvature is:

$$\kappa = \nabla \cdot \boldsymbol{n} \, . \tag{5}$$

The delta Dirac function is the most complex parameter to be determined numerically. The function is zero everywhere, except on the interface, calculated as:

$$\delta_d = |\nabla f| \, . \tag{6}$$

Note that Eq. 6 is indeed a consistent approximation of a Dirac delta function according with Brackbill *et al.* (1992) and Popinet (2018). The parametric analyse consist to turn the governing equations independent of the geometric and operational parameters of the problem. The dimensionless numbers are the most important parameters to analyse in this occasion. First of all, we define the dimensionless groups:

$$\rho' = \frac{\rho}{\rho_o}; \quad \mu' = \frac{\mu}{\mu_o}; \quad \boldsymbol{u}' = \frac{\boldsymbol{u}}{U}; \quad \nabla' = d_p \nabla; \quad \kappa' = d_p \kappa; \quad \delta_d' = d_p \delta_d; \quad t' = \frac{t}{\rho_o d_p^2 / \mu_o}; \quad P' = \frac{P}{\mu_o U / d_p} \, . \tag{7}$$

With the dimensionless parameters, the momentum equation can be rewritten as:

$$\left[f + (1-f)\frac{1}{N_\rho} \right] \left(\frac{\partial \boldsymbol{u}'}{\partial t'} + Re \, \boldsymbol{u}' \cdot \nabla' \boldsymbol{u}' \right) = -\boldsymbol{\nabla}' P' + \nabla' \cdot \left\{ \left[f + (1-f)\frac{1}{N_\mu} \right] \left(\nabla' \boldsymbol{u}' + \nabla' \boldsymbol{u}'^T \right) \right\} + \frac{1}{Ca} \kappa' \delta_d' \boldsymbol{n} \, , \tag{8}$$

in which $Re = \rho_1 U \sqrt{k} / \mu_1$ is the Reynolds number, $Ca = \sigma U / \mu_1$ is the capillary number, $N_\rho = \rho_1 / \rho_2$ is the density ratio and $N_\mu = \mu_1 / \mu_2$ is the viscosity ratio. We study the specific case that $N_\rho = 1$ and $Re << 1$ (Creeping flow), therefore, the dimensionless momentum equation can be overwrite as:

$$\frac{\partial \boldsymbol{u}'}{\partial t'} = -\boldsymbol{\nabla}' P' + \nabla' \cdot \left\{ \left[f + (1-f)\frac{1}{N_\mu} \right] \left(\nabla' \boldsymbol{u}' + \nabla' \boldsymbol{u}'^T \right) \right\} + \frac{1}{Ca} \kappa' \delta_d' \boldsymbol{n} \, . \tag{9}$$

On Eq. 9, it is possible to note that the viscosity ratio, N_μ, and the Capillary number, Ca, are the dimensionless numbers that influence on the recovery process. We evaluate the viscosity ratio range $0.01 \leq N_\mu \leq 100$ and Capillary number $0.02 \leq Ca \leq \infty$.

The numerical model evaluated is a simplified 2D micro-scale porous media and was used in order to study the influence of the Viscosity ratio (N_μ) and the Capillary number (Ca) on recovery efficiency. Two geometries were applied on the simulations, the homogeneous one (left on Fig 1) and the heterogeneous one (right on Fig. 1). The spheres are equal spaced forming a Lattice Boltzmann fractal. In the Heterogeneous geometry, the spheres reduce with the height (y position), but keeping the same porosity of the homogeneous one ($\phi = 0.7$).

The Basilisk© software use cartesian adaptative meshes, becoming possible to refine the mesh on critical regions, such as the fluids interface and solid boundaries (as shown on left side of Fig. 1). The mesh is defined by levels and the number of cells per dimension (1D, 2D or 3D) is given by 2^n, where n is level of refinement. For example, if a 2D square domain is discretized with a fixed refinement level 8, each direction will contain 256 cells, then the whole domain will contain 65,536 cells.

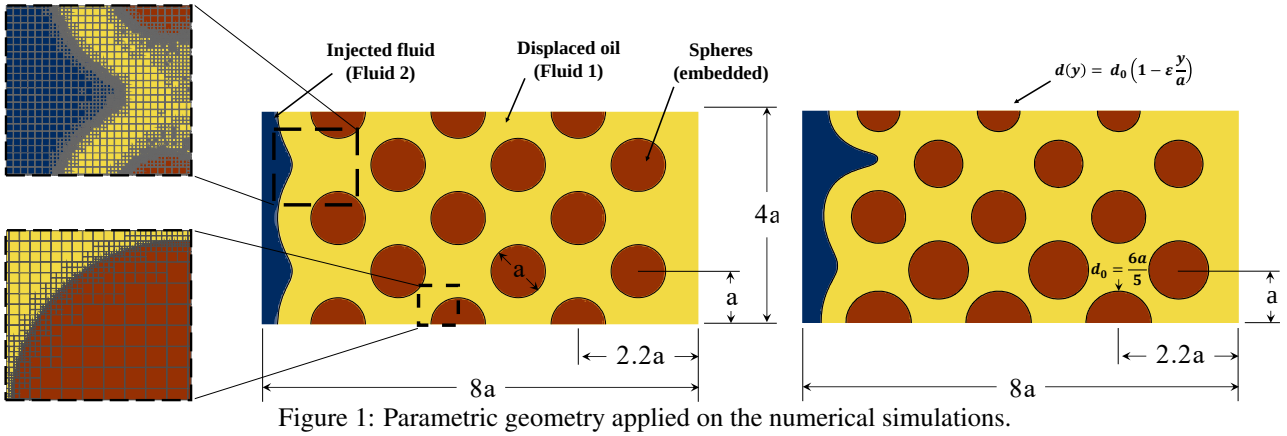

Figure 1: Parametric geometry applied on the numerical simulations.

Initially, the domain is fully saturated with the fluid to be displaced, Fluid 1 (yellow), and Fluid 2 (blue) is injected on the left side of the domain, displacing the Fluid 1. The top and bottom sections have free slip condition on the tangential direction and null normal velocity component. The right section have relative pressure 0 Pa and the spheres have no slip condition.

Due the complexity of the flow, some stability criteria needs to be considered. The first of all, the Courant number, Co, is a criteria to time-explicit solvers, calculated as:

$$Co = \frac{u_l \Delta t}{\Delta x} \, . \tag{10}$$

u_l is the local velocity, Δx is the mesh length and Δt the time step. The Courant number to the solver stability needs to be $Co \leq 0.5$. Dealing with a interfacial flow, the time-step also needs to be smaller than the oscillation period of the smallest capillary wave:

$$\Delta t \leq \sqrt{\frac{\rho_m \Delta x^3}{\pi \sigma}} \, , \tag{11}$$

in which $\rho_m = (\rho_1 + \rho_2)/2$ is the average density of the fluids. The simulations were performed on a Desktop Intel Core i7-4770 CPU 3.40GHz 16GB RAM. The output parameters analyses were the finger formation, the liquid film trapped on the porous grains and the lost mass (m_e) as global parameter to analyse the recovery efficiency, calculated by:

$$m_e = \frac{mass\ of\ Fluid\ 1\ entrapped\ in\ the\ porous\ media}{total\ mass\ of\ fluid\ in\ the\ porous\ media} \, , \tag{12}$$

i. e., the most efficient recovery process presents a minimum lost mass. The values of m_e were evaluated on the breakthrough time, defined by the time in which the injected fluid (blue) reaches the outlet section (right side of the domain).

3. RESULTS AND DISCUSSIONS

3.1 Mesh independence test

The front interface and the lost mass fraction were used as the interested parameters to the independence test. With a low refinement level, the fluids interface is rough, and with the increase of the refinement level, the interface tends to become smooth. The minimum level 7 was fixed in all cases on the mesh independence tests, and the maximum level range from 8 to 12. The mesh is refined according the residual of each selected variable, and to this study the mesh is refined according the volume fraction (f), the fluid-solid interface and the velocity field.

As shown in Fig. 2, the interface with maximum level of refinement 9 is rough. Its quality is significantly improved with maximal level 10. The interface is smooth in such a case. The fraction mass m_e changes a lot from maximum level 9 to 10. It is 0.5 in the first case and decreases to 0.4 in the second, reduction of 20%. The difference between the maximum level 10 and 11 is not significant. The shape of the interface is almost the same and the fraction m decreases less than 2%. Since the computational time increase a lot with the maximum level 11 instead of 10, it is considered that the maximum level 10 is sufficient to this case. This process was made for each viscosity ratio.

3.2 Influence of Viscosity ratio and Capillary number on the recovery process

Fig. 3 shows the interface at the breakthrough time to the homogeneous porous media. On the first column it is possible to see that on homogeneous porous media, the injected fluid passes through all the pores of the media, independently of N_μ to $Ca = \infty$, but the breakthrough is faster for larger viscosity ratios, i.e., the interface front delays when the viscosity of the displacing liquid increases, been able to drag more fluid.

As seen on Fig. 3, the displacement patters changes a lot with the entire range of viscosity ratio, but some results are similar. The amount of entrapped liquid decreases from the most significant viscosity ratio analysed ($N_\mu = 40$) to the minimal ($N_\mu = 0.5$). Analysing the entrapped liquid and the fingers, precisely, the tip of the interface front for the values of viscosity ratio, in the first column of the figure, it is possible to see that the amount of liquid around the spheres that compose the porous media from the top to the bottom is significant for $N_\mu = 40$ and almost absent for $N_\mu = 0.5$, especially on the first spheres from left to right. It is worth noting that the tip of the interface becomes thinner when N_μ decreases, this was also discussed by Soares and Thompson (2009); Soares *et al.* (2015); Caliman *et al.* (2017). Hence, the improvement of recovery efficiency obtained with a reduction of N_μ is because the drag force increase and not properly by the displacement.

Analysing the effects of Ca on Fig. 3, the decrease of the Ca make the tip thicker by the increase of the surface tension. The higher the surface tension the higher the bending resistance on the fluids interface. Due to that, the fingers are formed even against the flow, failing to swept some pores, especially at high N_μ, as observed by Lenormand *et al.* (1988);Zhang *et al.* (2011);Tsuji *et al.* (2016) and Hu *et al.* (2020).

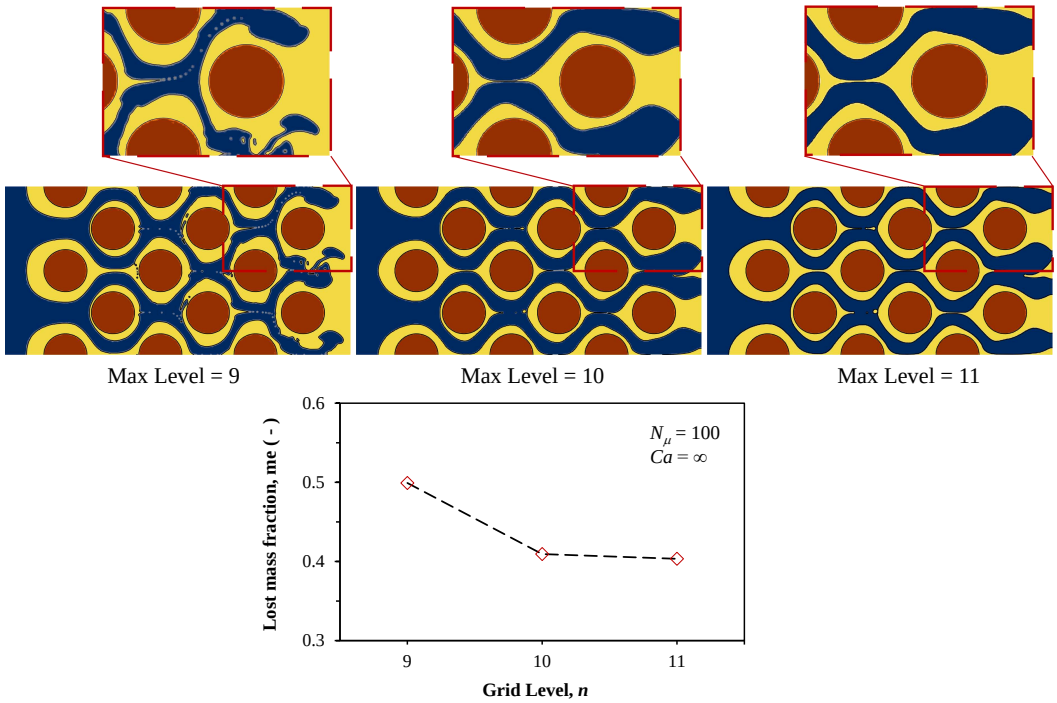

Figure 2: Mesh validation with $Ca = \infty$ and $N_\mu = 100$.

Fig. 4 shows the displacing liquid penetration into the heterogeneous porous media to the evaluated cases. The first row shows the results for a range of viscosity ratio $0.01 \leq N_\mu \leq 20$ at fixed a capillary number, $Ca = \infty$. For the entire range of viscosity ratio, the sweep process is non-uniform. The displacing liquid tends to flow through the region with less resistance, where the porous are larger, at the top side of the domain. Such a preferential path implies a faster breakthrough when compared with the homogeneous media. For $N_\mu = 20$, the breakthrough time to heterogeneous porous media is around 75% of the breakthrough time to the homogeneous porous media to the same viscosity ratio. It is also possible to note that the the sweep increase with the reduction of N_μ. A thinner tip of finger penetrates easier in the pores, increasing the sweep of the injected fluid. The effects of Ca in Fig. 4 are the same as those observed to the homogeneous porous media, increasing the recovery factor due a thicker tip.

Fig. 5 show the lost mass fraction for the homogeneous and heterogeneous cases at $Ca = \infty$. It is noted that the displacement occurs at three regions. For low viscosity ratios, the viscous forces imposed by the injected fluid domain the displacement and the lost mass is almost constant. With the increase of N_μ, the lost mass fraction also increases, due to the increase of the viscous forces of the recovered fluid, that dispute with the forces imposed by the injected fluid. As the viscous forces further increases, the viscous forces imposed by the recovered fluid dominates the displacement and the lost mass return to another constant plateau.

In both porous media, the increase of N_μ increase the lost mass fraction. It is also noted in Fig. 5 that the lost mass fraction for the heterogeneous porous media is always higher than the homogeneous porous media. But the lower plateau of lost mass to both cases are almost the same, but the heterogeneous porous media reaches this plateau in a lower N_μ when compared to the homogeneous case. Fig. 6a and Fig. 6b show the influence of Ca on the lost mass fraction to the homogeneous and heterogeneous porous media, respectively.

As it is possible to see in Fig. 6a, to all the range of N_μ, that the reduction of Ca reduces the lost mass fraction. The thicker tip drag more fluid during the pores sweep and also help the efficiency of the process. On Fig. 6b, it is possible to note the same behaviour of the homogeneous porous media is seen on heterogeneous porous media. This behaviour was also observed by Zhang *et al.* (2011); Gu *et al.* (2018) and Soares (2015). Some authors such as Lenormand *et al.* (1988) and Hu *et al.* (2020) observed a different behaviour of the capillary number effects. For high viscosity ratio, the decrease of the capillary number reduces the lost mass, i.e., the transit from viscous finger to capillary finger increase the displacement efficiency. But, to low viscosity ratio, the reduction of Ca increases the lost mass fraction, indicating that transit from a stable displacement to a capillary finger reduces the displacement efficiency.

Although some authors comes to different conclusions about the effects of the capillary number on the fluid displacement, there are some aspects to be considered. Zhang *et al.* (2011) and Soares (2015) use simplified geometry on the analyse, such as capillary tube or porous media with grains with a constant diameter and equally spaced to compose the porous media. In contrast, Lenormand *et al.* (1988); Hu *et al.* (2020) study models closed to the reality, with a grain distribution and a aleatory spaced grains (tortuous) porous media. The tortuosity can make some small pores difficult to be penetrated

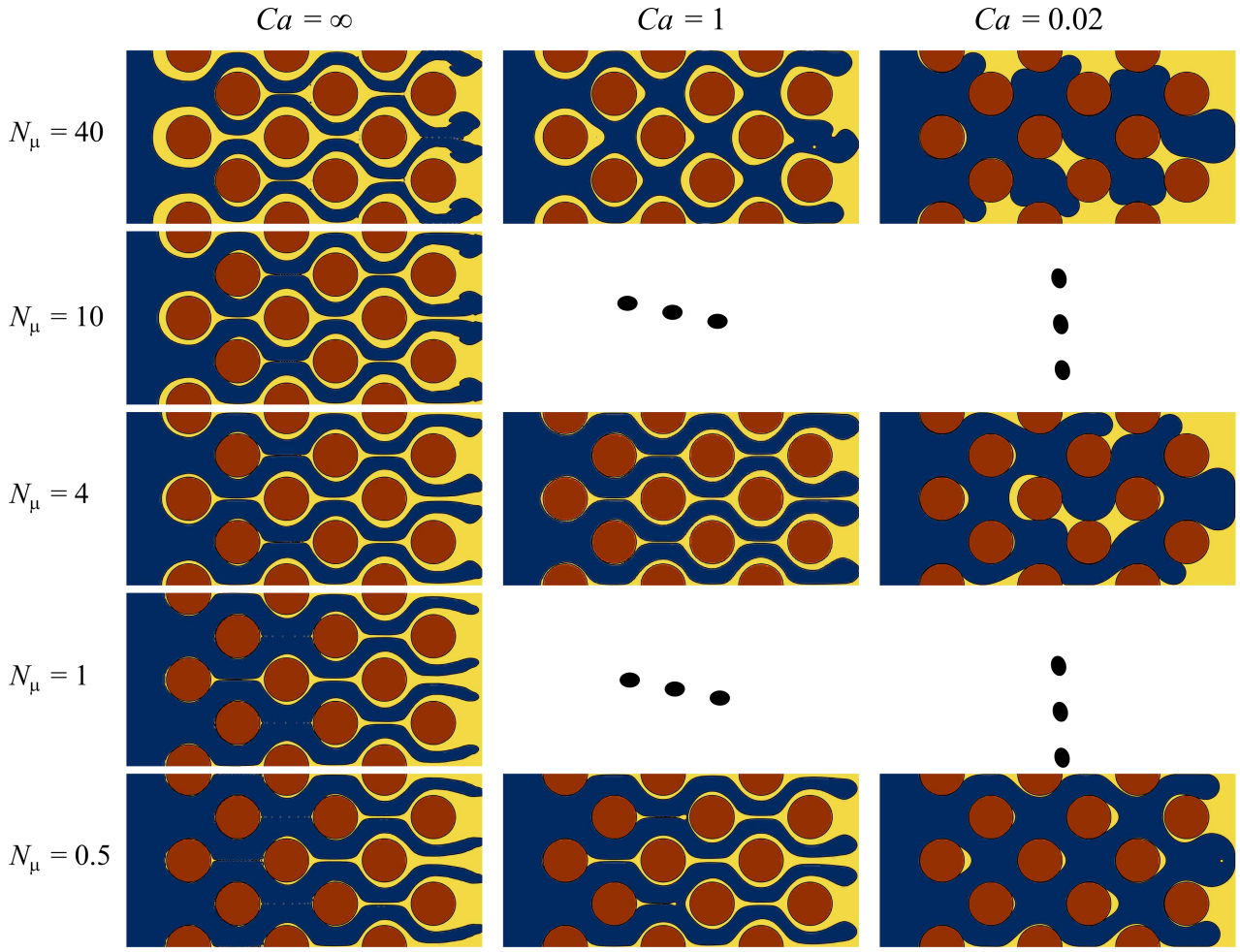

Figure 3: Displacement pattern to the range of N_μ and Ca to the homogeneous porous media.

by the injected fluid with a high surface tension (thicker tip). Due to that, the reduction of the capillary number, even with a low N_μ, can reduce the pores sweep, reducing the displacement efficiency.

4. CONCLUSIONS

This study evaluate the influence of Ca and N_μ on the displacement efficiency on homogeneous and heterogeneous porous media. It is observed that the reduction of the viscosity ratio, i.e., the injection of a more viscous fluid on the porous media, increase the recovery efficiency in the both cases. Besides some divergences on the literature about the capillary number effects, the present work observed the reduction of the lost mass with the reduction of Ca, resulting on a increase of the recovery efficiency. The next steps of our study will be the evaluation of a tortuous porous media in order to compare the results of an homogeneous porous media with a heterogeneous tortuous porous media to evaluate the effects of Ca on this scenario, and evaluate if the tortuosity is the parameter that define if the capillary number increases or reduces the displacement efficiency.

5. ACKNOWLEDGEMENTS

The authors thanks the Instituto Federal do Espírito Santo (IFES) and the Universidade Federal do Espírito Santo (UFES) for the resources to carry the research and FAPES for the financial support to the development of this research.

6. REFERENCES

Brackbill, J., Kothe, D. and Zemach, C., 1992. "A continuum method for modeling surface tension". *Journal of Computational Physics*, Vol. 100, No. 2, pp. 335–354. doi:10.1016/0021-9991(92)90240-y. URL `https://doi.org/10.1016/0021-9991(92)90240-y`.

Caliman, H.M., Soares, E.J. and Thompson, R.L., 2017. "An experimental investigation on the Newtonian–Newtonian and

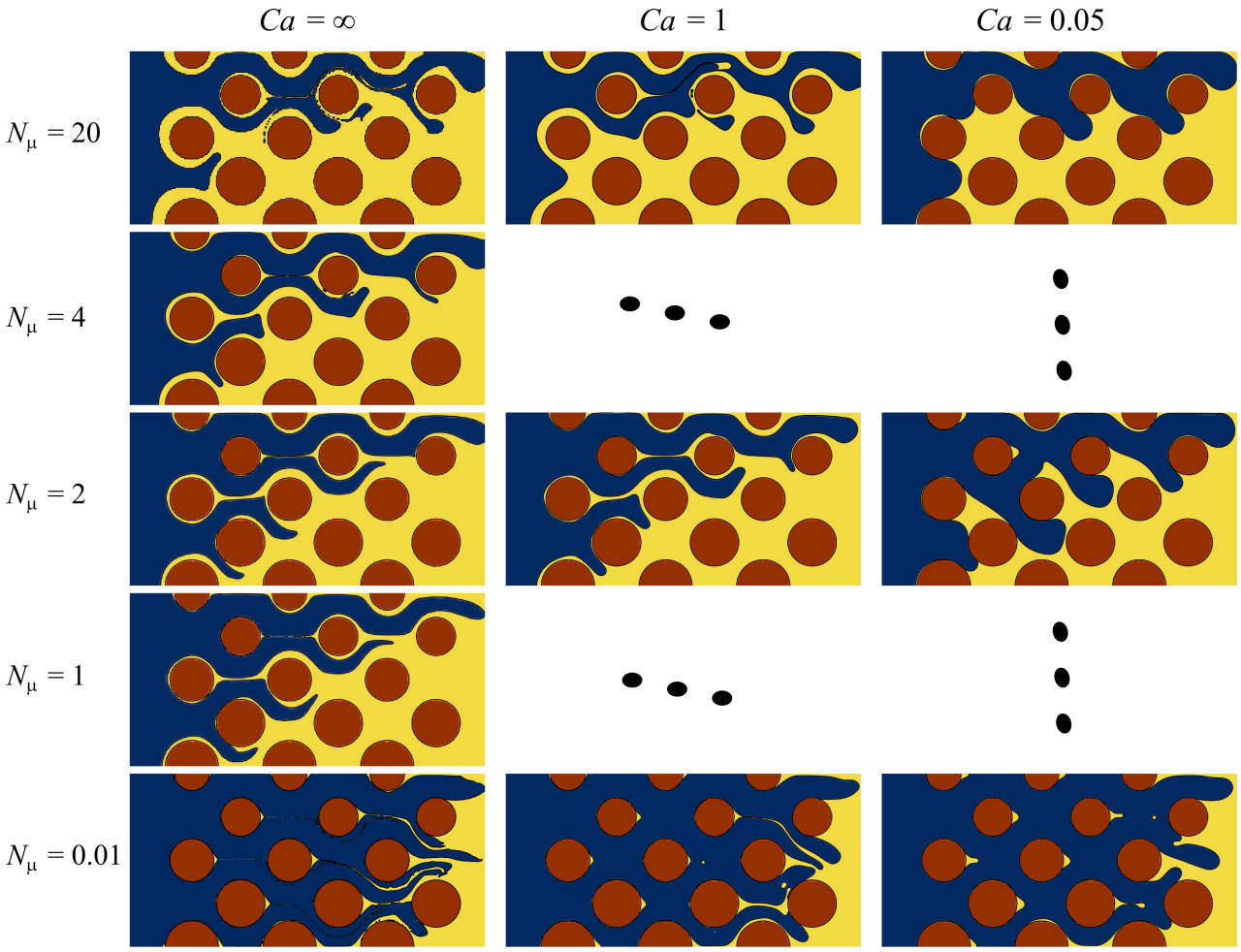

Figure 4: Displacement pattern to the range of N_μ and Ca to the heterogeneous porous media.

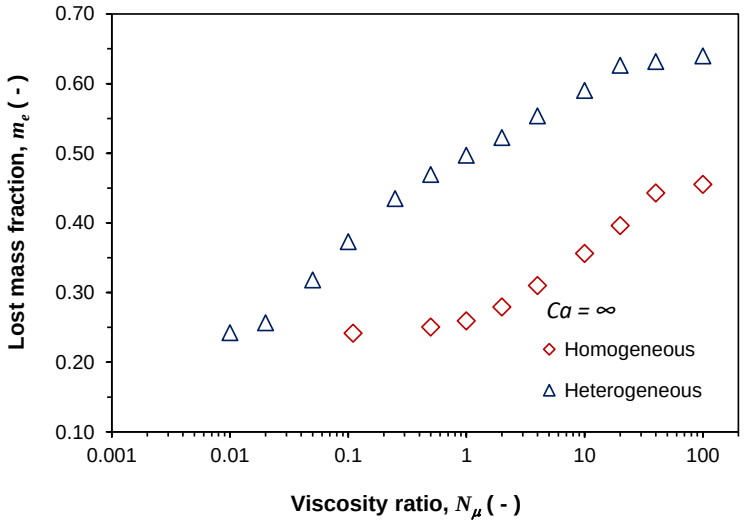

Figure 5: Influence of N_μ on the lost mass fraction (m_e) to the homogeneous and heterogeneous porous media with $Ca = \infty$.

viscoplastic–Newtonian displacement in a capillary tube". *J. non-Newt. Fluid Mech.*, Vol. 247, pp. 207–220.

Deka, H., Pierson, J.L. and Soares, E.J., 2019. "Retraction of a viscoplastic liquid sheet". *Journal of Non-Newtonian Fluid Mechanics*, Vol. 272, p. 104172.

Deka, H., Pierson, J.L. and Soares, E.J., 2020. "Retraction criteria of viscoplastic drops and sheets: Long-wave approxima-

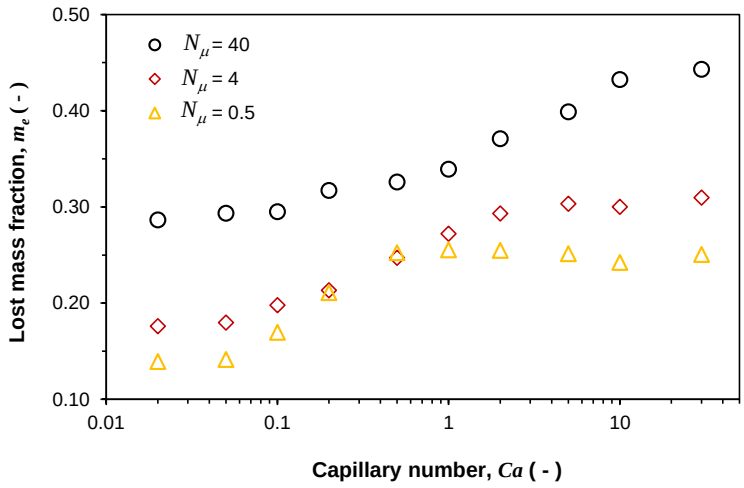

(a)

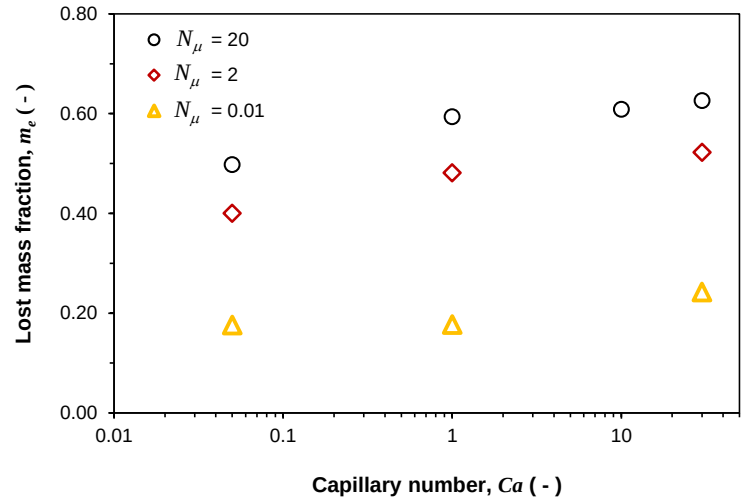

(b)

Figure 6: Influence of Capillary number (Ca) on the lost mass fraction (m_e) on (a) the heterogeneous porous media and (b) the heterogeneous porous media.

tions". *Journal of Non-Newtonian Fluid Mechanics*, Vol. 284, p. 104352.

Deoclecio, L.H.P., Soares, E.L., Deka, H. and Pierson, J.L., 2021. "Bubble entrapment condition in bingham materials". *J, Non-Newtonian Fluid Mechanics*, Vol. 295, p. 104616.

Dias, M.M. and Payatakes, A.C., 1986. "Network models for two-phase flow in porous media part 1. immiscible microdisplacement of non-wetting fluids". *J. Fluid Mech.*, Vol. 164, pp. 305–336.

Fathi, S.J., Austad, T. and Strand, S., 2011. "Water-based enhanced oil recovery (eor) by "smart water":optimal ionic composition for eor in carbonates". *Ernery and Fuels*, Vol. 25, pp. 5173–5179.

Gu, Q., Liu, H. and Zhang, Y., 2018. "Lattice boltzmann simulation of immiscible two-phase displacement in two-dimensional berea sandstone". *Applied Sciences*, Vol. 8, No. 9, p. 1497. doi:10.3390/app8091497.

Hu, Y., Patmonoaji, A., Zhang, C. and Suekane, T., 2020. "Experimental study on the displacement patterns and the phase diagram of immiscible fluid displacement in three-dimensional porous media". *Advances in Watter Resources*, Vol. 140, p. 103584.

Johansen, H. and Colella, P., 1998. "A cartesian grid embedded boundary method for poisson's equation on irregular domains". *Journal of Computational Physics*, Vol. 147, No. 1, pp. 60–85. doi:10.1006/jcph.1998.5965.

Lagrée, P.Y., Staron, L. and Popinet, S., 2011. "The granular column collapse as a continuum: validity of a two-dimensional navier-stokes model with a $\mu(i)$-rheology". *Journal of Fluid Mechanics*, Vol. 686, p. 378.

Lenormand, R., Touboul, E. and Zarcone, C., 1988. "Numerical models and experiments on immiscible displacements in porous media". *J. Fluid Mech*, Vol. 189, pp. 165–187.

Needham, R.B. and Doe, P.H., 1987. "Polymer flooding review". *J. Petroleum Tech.*, Vol. 39, pp. 1503–1507.

Pierson, J.L., Magnaudet, J., Soares, E.J. and Popinet, S., 2020. "Revisiting the taylor-culick approximation: Retraction of

an axisymmetric filament". *Phys. Rev. Fluids*, Vol. 5, p. 073602.

Popinet, S., 2009. "An accurate adaptive solver for surface-tension-driven interfacial flows". *Journal of Computational Physics*, Vol. 228, No. 16, pp. 5838–5866.

Popinet, S., 2015. "A quadtree-adaptive multigrid solver for the serre–green–naghdi equations". *Journal of Computational Physics*, Vol. 302, pp. 336–358.

Popinet, S., 2018. "Numerical models of surface tension". *Annual Review of Fluid Mechanics*, Vol. 50, pp. 49–75.

Shende, T., Niasar, V. and Babaei, M., 2021. "Pore-scale simulation of viscous instability for non-newtonian two-phase flow in porous media". *J. non-Newt. Fluid Mech.*, Vol. 296, p. 104628.

Soares, E..J., Thompson, R.L. and Niero, D.C., 2015. "Immiscible liquid–liquid pressure-driven flow in capillary tubes: experimental results and numerical comparison". *Phys. Fluids*, Vol. 27, p. 082105.

Soares, E.J., 2015. "On the transient behaviour of the drag reducing flows". *ERCOFTAC Bulletin*, Vol. 104, pp. 19–23.

Soares, E.J., Carvalho, M.S. and de Souza Mendes, P.R., 2005. "Immiscible liquid-liquid displacement in capillary tubes". *Journal of Fluids Engineering*, Vol. 127, No. 1, pp. 24–31.

Soares, E.J. and Thompson, R.L., 2009. "Flow regimes for the immiscible liquid-liquid displacement in capillary tubes with complete wetting of the displaced liquid". *J. Fluid Mech.*, Vol. 641, pp. 63–84.

Taylor, G.I., 1960. "Deposition of a viscous fluid on a plane surface". *J. Fluid Mech.*, Vol. 9, pp. 8–14.

Taylor, G.I., 1961. "Deposition of a viscous fluid on the wall of a tube". *J. Fluid Mech.*, Vol. 10, pp. 161–165.

Tsuji, T., Jiang, F. and Christensen, K.T., 2016. "Characterization of immiscible fluid displacement processes with various capillary numbers and viscosity ratios in 3d natural sandstone". *Advances in Watter Resources*, Vol. 000, pp. 1–13.

Zhang, C., Oostrom, M., Witsma, T.W., Grate, J.W. and Warner, M.G., 2011. "Influence of viscous and capillary forces on immiscible fluid displacement: Pore-scale experimental study in a water-wet micromodel demonstrating viscous and capillary fingering". *Energy & Fuels*, Vol. 25, pp. 3493–3505.

Zhong, H., Li, Y., Zhang, W., Yin, H., Lu, J. and Guo, D., 2018. "Microflow mechanism of oil displacement by viscoelastic hydrophobically associating water-soluble polymers in enhanced oil recovery". *Polymer*, Vol. 10, p. 628.

7. RESPONSIBILITY NOTICE

The authors are solely responsible for the printed material included in this paper.